ORIGINAL RESEARCH

The Innate Immune Protein S100A9 Protects from T-Helper Cell Type 2–mediated Allergic Airway Inflammation

Lauren D. Palmer[1,2], K. Nichole Maloney[1,2], Kelli L. Boyd[1,2], A. Kasia Goleniewska[2,3], Shinji Toki[2,3], C. Noel Maxwell[4,5], Walter J. Chazin[2,4,5], R. Stokes Peebles, Jr.[1,2,3], Dawn C. Newcomb[1,2,3], and Eric P. Skaar[1,2]

[1]Department of Pathology, Microbiology, and Immunology, [2]Vanderbilt Institute for Infection, Immunology and Inflammation, and [3]Division of Allergy, Pulmonary, and Critical Care Medicine, Department of Medicine, Vanderbilt University Medical Center, Nashville, Tennessee; and [4]Department of Biochemistry and [5]Department of Chemistry, Center for Structural Biology, Vanderbilt University, Nashville, Tennessee

ORCID IDs: 0000-0001-7458-6129 (L.D.P.); 0000-0003-4379-9118 (S.T.); 0000-0002-2180-0790 (W.J.C.); 0000-0002-1429-7875 (R.S.P.); 0000-0001-5094-8105 (E.P.S.).

Abstract

Calprotectin is a heterodimer of the proteins S100A8 and S100A9, and it is an abundant innate immune protein associated with inflammation. In humans, calprotectin transcription and protein abundance are associated with asthma and disease severity. However, mechanistic studies in experimental asthma models have been inconclusive, identifying both protective and pathogenic effects of calprotectin. To clarify the role of calprotectin in asthma, calprotectin-deficient *S100A9*$^{-/-}$ and wild-type (WT) C57BL/6 mice were compared in a murine model of allergic airway inflammation. Mice were intranasally challenged with extracts of the clinically relevant allergen, *Alternaria alternata* (Alt Ext), or PBS every third day over 9 days. On Day 10, BAL fluid and lung tissue homogenates were harvested and allergic airway inflammation was assessed. Alt Ext challenge induced release of S100A8/S100A9 to the alveolar space and increased protein expression in the alveolar epithelium of WT mice. Compared with WT mice, *S100A9*$^{-/-}$ mice displayed significantly enhanced allergic airway inflammation, including production of IL-13, CCL11, CCL24, serum IgE, eosinophil recruitment, and airway resistance and elastance. In response to Alt Ext, *S100A9*$^{-/-}$ mice accumulated significantly more IL-13^{+}IL-5^{+}CD4^{+} T-helper type 2 cells. *S100A9*$^{-/-}$ mice also accumulated a significantly lower proportion of CD4^{+} T regulatory (Treg) cells in the lung that had significantly lower expression of CD25. Calprotectin enhanced WT Treg cell suppressive activity *in vitro*. Therefore, this study identifies a role for the innate immune protein, S100A9, in protection from CD4^{+} T-helper type 2 cell hyperinflammation in response to Alt Ext. This protection is mediated, at least in part, by CD4^{+} Treg cell function.

Keywords: CD4^{+} T cells; knockout mouse; allergic airway inflammation; S100A9; calprotectin

Calprotectin is an innate immune protein associated with inflammatory diseases. It comprises approximately 50% of the neutrophil cytoplasm, but is also produced by other myeloid cells, epithelial cells, and some endothelial cells (1). Notably, calprotectin is a major component of the peripheral blood eosinophil proteome (2). Calprotectin is a heterodimer of S100A8 (myeloid-related protein [MRP] 8) and S100A9 (MRP14) that binds metals and has bacteriostatic and proinflammatory activity (3, 4). The proinflammatory activity of calprotectin is thought to be mediated by its role as a damage-associated molecular pattern (DAMP) that promotes inflammation as a ligand for the receptor for advanced glycation end products (RAGE) and Toll-like receptor-4 (5–7).

Transcriptional and proteomic studies have linked calprotectin levels to asthma. The transcripts for *S100A8* and *S100A9* were among the most highly upregulated in peripheral blood mononuclear cells of children with asthma compared with control subjects without asthma (8). Furthermore, calprotectin is more abundant in induced sputum from patients with

(Received in original form July 1, 2018; accepted in final form April 3, 2019)

Supported by American Asthma Foundation funds (E.P.S.), National Institutes of Health grants R01 AI101171 (E.P.S. and W.J.C.), F32 AI122516 (L.D.P.), T32 HL094296 to Dr. Timothy Blackwell (L.D.P.), R01 HL122554 (D.C.N.), R21 AI121420 (D.C.N.), R01 U19AI095227 (R.S.P.), R01 AI124456 (R.S.P.), R01 AI145265 (R.S.P.), R01 AI111820 (R.S.P.), and U.S. Department of Veterans' Affairs grant I01BX004299 (R.S.P.).

Author Contributions: Conception and design—L.D.P., K.N.M., K.L.B., S.T., R.S.P., D.C.N., and E.P.S.; acquisition of data—L.D.P., K.N.M., K.L.B., A.K.G., C.N.M., W.J.C., and D.C.N.; analysis and interpretation of data—L.D.P., K.N.M., K.L.B., S.T., R.S.P., D.C.N., and E.P.S.; drafting the manuscript—L.D.P., K.N.M., K.L.B., R.S.P., D.C.N., and E.P.S.; critical revisions—L.D.P., K.N.M., K.L.B., A.K.G., S.T., C.N.M., W.J.C., R.S.P., D.C.N., and E.P.S.

Correspondence and requests for reprints should be addressed to Eric P. Skaar, Ph.D., M.P.H., Vanderbilt University Medical Center, Department of Pathology, Microbiology, and Immunology, MCN A-5301, Nashville, TN 37232-2363. E-mail: eric.skaar@vumc.org.

This article has a data supplement, which is accessible from this issue's table of contents at www.atsjournals.org.

Am J Respir Cell Mol Biol Vol 61, Iss 4, pp 459–468, Oct 2019
Copyright © 2019 by the American Thoracic Society
Originally Published in Press as DOI: 10.1165/rcmb.2018-0217OC on April 3, 2019
Internet address: www.atsjournals.org

asthma compared with healthy control subjects (9). Among patients with asthma, calprotectin is associated with severe disease. Calprotectin is enriched in patients with uncontrolled asthma and neutrophilic-type sputum (10, 11). Combined, these findings suggest that calprotectin is important in regulating airway inflammation that is associated with asthma.

Mechanistic studies using experimental asthma models have implicated calprotectin in opposing roles, both promoting and protecting from allergic airway inflammation (AAI). In a murine model of adaptive AAI using ovalbumin (OVA), exogenous application of S100A8 protein reduced mast cell degranulation, production of the type 2 cytokine, IL-13, and production of eosinophil chemoattractants, suggesting that calprotectin is protective (12). Similarly, in a rat model of acute OVA challenge, exogenous S100A9 was protective and reduced pulmonary resistance (13). In contrast, neutralizing anti-S100A8 and anti-S100A9 antibodies decreased total cellular recruitment in mice challenged with *Aspergillus* allergens mixed with OVA (14), suggesting that calprotectin promotes AAI. In addition, exogenous S100A9 promoted neutrophil recruitment and anti-S100A9 neutralizing antibodies abrogated AAI in response to OVA/complete Freund's adjuvant treatment (11). Exogenous application of calprotectin also promoted release of TSLP and IL-25 when normal human bronchial epithelial cells were challenged with the extracts from the allergenic mold, *Alternaria alternata* (Alt Ext) (15). Consistent with a role for calprotectin in promoting AAI, mice lacking the calprotectin receptors, Toll-like receptor-4 and RAGE, have reduced AAI when challenged with Alt Ext or house dust mite extract (16, 17). Taken together, these data suggest that the role for calprotectin in AAI warrants further investigation.

To clarify the role of calprotectin in asthma, calprotectin-deficient *S100A9*$^{-/-}$ mice were tested in a murine model of acute AAI using Alt Ext. *S100A9*$^{-/-}$ mice do not express S100A8 in peripheral blood cells or in the spleen, and are therefore calprotectin deficient (18). In addition, *S100A9*$^{-/-}$ neutrophils are defective at upregulating CD11b in response to IL-8, in responding to chemotactic stimuli *in vitro*, and in migration to the hearts of mice infected with *Staphylococcus aureus* (18, 19). *S100A9*$^{-/-}$ mice are defective in controlling infection by *Acinetobacter baumannii*, *S. aureus*, *Listeria monocytogenes*, *Klebsiella pneumoniae*, and *Helicobacter pylori* (20–23). AAI in *S100A9*$^{-/-}$ mice has not been previously reported.

Alt Ext causes AAI and asthma exacerbations in sensitized people (24). In murine models, Alt Ext induces robust T-helper (Th) type 2 responses, including type 2 cytokine production by group 2 innate lymphoid cells (ILC2s) and CD4^{+} T-helper (Th) type 2 cells, eosinophilic recruitment, and airway hyperresponsiveness (AHR) (16, 25–31). We used a 10-day model of Alt Ext challenge to investigate the effects of calprotectin on innate and adaptive type 2 AAI responses, including function of epithelial cells, ILC2s, CD4^{+} Th2 cells, and eosinophils. Our results demonstrate that, in this model, wild-type (WT) mice upregulate calprotectin in response to Alt Ext challenge, whereas calprotectin-deficient mice have increased AAI in response to Alt Ext challenge, as measured by increased IL-13, serum IgE, eosinophil recruitment, and AHR. Furthermore, these data suggest that increased AAI in calprotectin-deficient mice is due to enhanced CD4^{+} Th2 responses.

Methods

Mice

WT C57BL/6J mice were obtained from The Jackson Laboratory. *S100A9*$^{-/-}$ mice were generated in the C57BL/6 background (18), and backcrossed into C57BL/6J. *S100A9*$^{-/-}$ mice are 87% C57BL/6J and 13% C57BL/6NJ; littermate controls used in one experiment assessing T regulatory (Treg) cell numbers and marker expression were 92.5% C57BL/6J

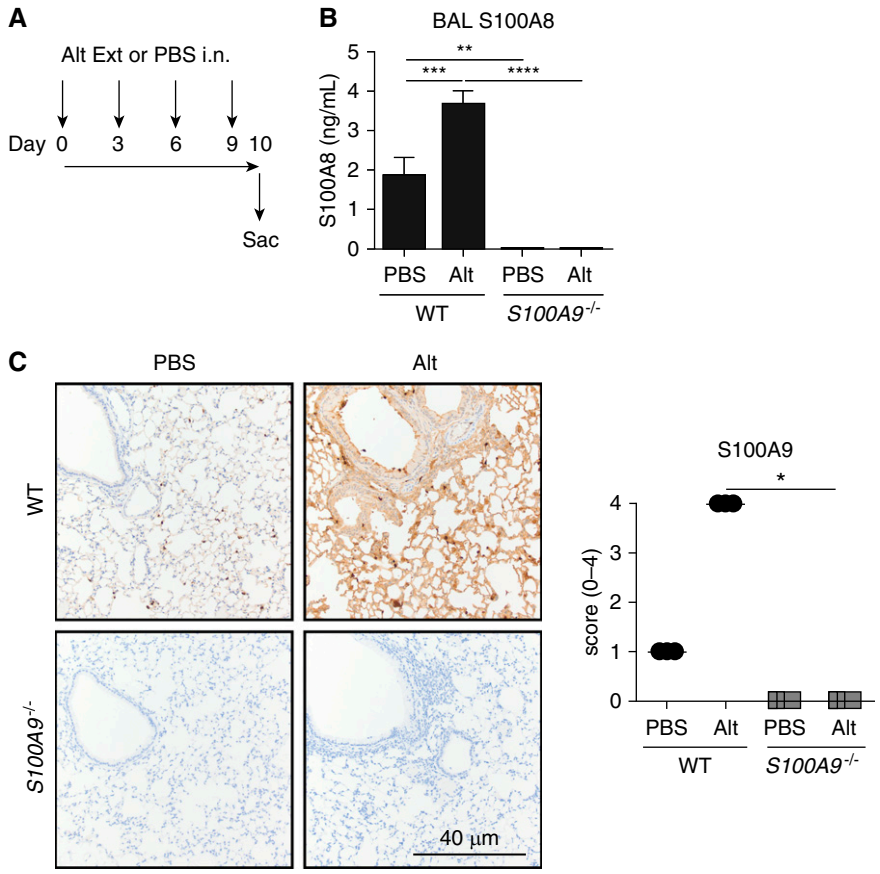

Figure 1. *Alternaria alternata* (Alt Ext [Alt]) challenge induces production of calprotectin in the lung. (*A*) Mice were intranasally (i.n.) challenged with Alt or mock challenged with PBS on Days 0, 3, 6, and 9, and killed on Day 10 at 24 hours after the final challenge. (*B*) S100A8 levels in the BAL were determined by ELISA; data are combined from three experiments and include 10–11 PBS-challenged and 15–21 Alt-challenged mice per group. (*C*) S100A9 production and distribution in the lungs were determined by immunohistochemistry. *$P < 0.05$, **$P < 0.01$, ***$P < 0.001$, and ****$P < 0.0001$. Scale bar: 40 μm. Data with error bars represent mean ± SEM. S100A9 = S100 calcium binding protein A9; Sac = killed; WT = wild-type.

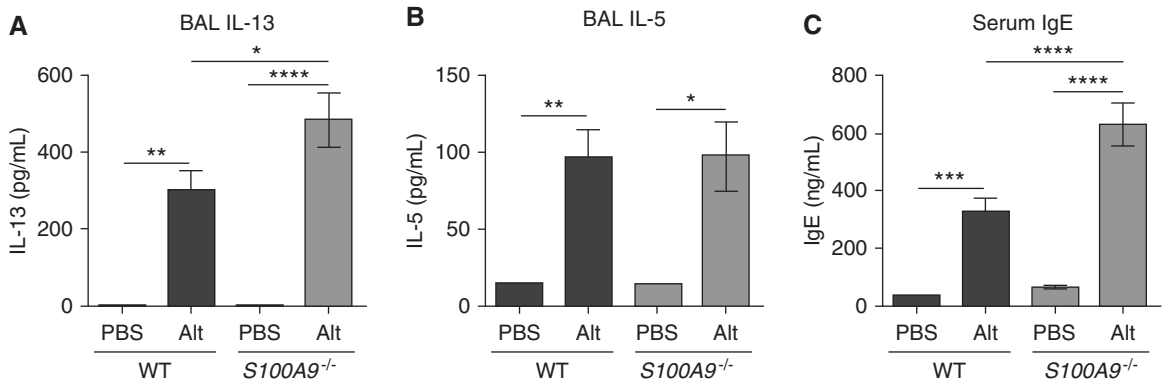

Figure 2. *S100A9*$^{-/-}$ mice produce more IL-13 and serum IgE in response to airway allergen challenge. (*A–C*) The level of BAL type 2 cytokines, IL-13 (*A*) and IL-5 (*B*), and serum IgE (*C*) were determined by ELISA. Data are combined from two separate experiments and include 11–17 Alt-challenged and eight or nine mock-challenged mice per genotype. *$P < 0.05$, **$P < 0.01$, ***$P < 0.001$, and ****$P < 0.0001$. Data with error bars represent mean ± SEM.

and 6.5% C57BL/6NJ. Although *S100A8*$^{-/-}$ mice are fetally resorbed (32), *S100A9*$^{-/-}$ mice are viable (18). Age-matched 7- to 11-week-old male WT C57BL/6J mice and *S100A9*$^{-/-}$ mice were maintained in specific pathogen-free facility conditions. All animal experiments were reviewed and approved by the Vanderbilt University Medical Center Institutional Animal Care and Use Committee, and were conducted according to the guidelines for the Care and Use of Laboratory Animals prepared by the Institute of Laboratory Animal Resources, National Research Council.

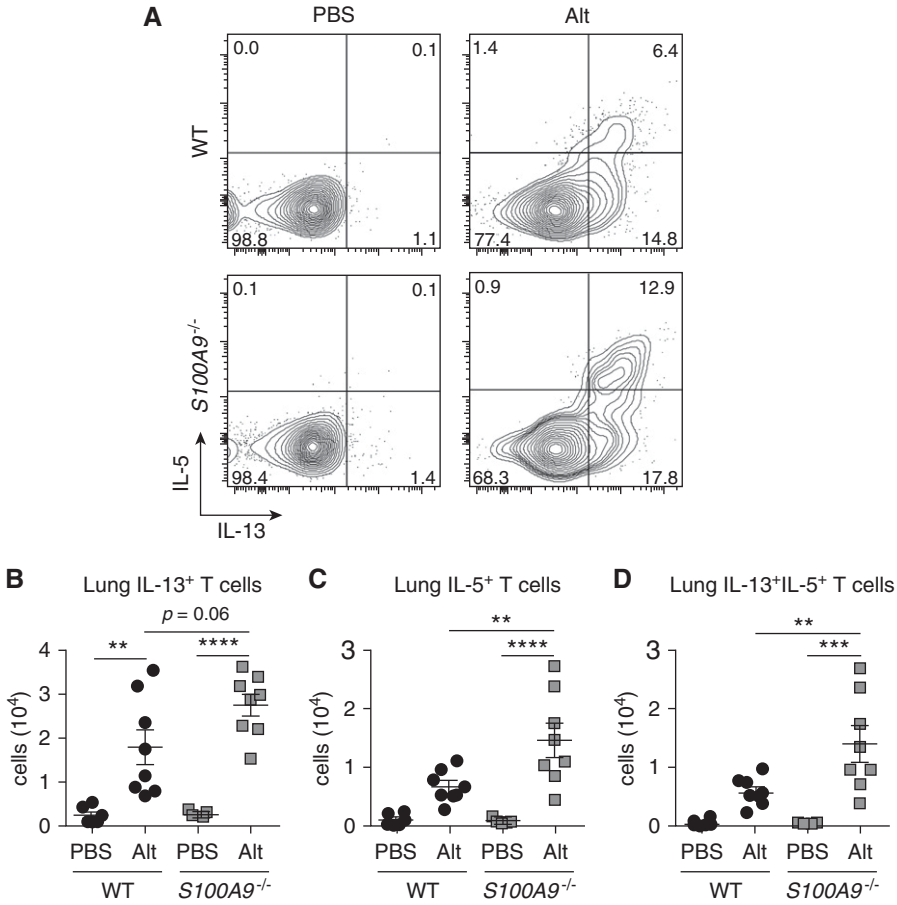

Figure 3. S100A9$^{-/-}$ mice more robustly activate and proliferate T-helper (Th) type 2 cells as a result of airway allergen challenge. (*A*) Representative flow plots with percentages of the parent CD3$^+$CD4$^+$ T cells shown. Aggregated data for the total number of (*B*) IL-13$^+$, (*C*) IL-5$^+$, and (*D*) IL-13$^+$IL-5$^+$ double-positive Th2 cells in the right lung. (*B–D*) Data are combined from two experiments and include eight Alt-challenged and five or six mock-challenged mice per genotype. **$P < 0.01$, ***$P < 0.001$, and ****$P < 0.0001$. Data with error bars represent mean ± SEM.

In Vivo Alt Ext Extract Challenge

WT and *S100A9*$^{-/-}$ mice were anesthetized with ketamine/xylazine and challenged intranasally with 7.5 μg protein content of Alt Ext (Greer Laboratories) in 80 μl PBS on Days 0, 3, 6, and 9. At 24 hours after the last challenge, mice were killed and tissues harvested. When indicated, BAL fluid was collected in 0.8 ml PBS for cytokine analysis and cell counting. Cells were cytocentrifuged onto glass slides, stained with Three-Step Stain Set (Richard Allen Scientific), and cell types were counted ($n = 200$) using standard morphological techniques as previously described (33).

Histopathology of Lungs

Lungs were inflated and fixed in 10% buffered formalin for 3–4 days before embedding in paraffin blocks. For detailed methods, *see* the data supplement.

Flow Cytometry

After BAL on Day 10 of the Alt Ext challenge protocol, IL-5– and IL-13–producing Th2 cells and ILC2s were quantified from right lungs. Detailed staining procedures are available in the data supplement.

Methacholine Challenge

AHR and airway elastance was measured on Day 10 after Alt Ext challenge. Detailed

methods are available in the data supplement.

Cytokine Measurements

ELISA kits (R&D Systems Inc.) were used to measure cytokine levels according to the manufacturers' instructions. Quantikine kits were used for IL-13, IL-5, TSLP, and IL-10, and Duoset kits were used for S100A8, CCL11, CCL24, IL-25 (IL-17E), and IL-33. Cytokines were measured from BAL, or whole lungs (post-BAL) were homogenized in 0.7 ml PBS using a Bullet Blender tissue homogenizer (Next Advance) and used to measure IL-25 and IL-10 or diluted eightfold to measure CCL11. Serum was diluted 100-fold and measured using a total IgE ELISA kit (BioLegend).

In Vitro Treg Cell Suppression Assay

$CD4^+$ Treg and $CD4^+$ effector cells were isolated from spleens and assessed for Treg suppression of $CD4^+$ effector cell proliferation. Detailed methods are available in the data supplement.

Statistical Analyses

Statistical analyses were performed with GraphPad Prism 6.0 (GraphPad Software Inc.) by one-way ANOVA with Sidak's multiple comparisons, unless indicated otherwise. Significance is indicated by asterisks seen in the figure legends; all P values less than 0.1 are reported. All data are represented as mean (±SEM). Data below the limit of detection were assigned to half the limit of detection for statistical purposes.

Results

S100A8 and S100A9 Are Produced at Increased Levels in WT Mice Challenged with Alt Ext

Based on previous studies associating the presence of calprotectin with severe asthma, we hypothesized that calprotectin would be present at higher levels in Alt Ext–challenged mice. To test this hypothesis, we used a 10-day model of allergic airway inflammation with the physiologically relevant allergen, Alt Ext (16). WT and *S100A9*$^{-/-}$ mice were challenged with Alt Ext on Days 0, 3, 6, and 9, and BAL and or lungs were harvested on Day 10 (Figure 1A). The levels of S100A8 in the BAL of Alt Ext–challenged mice were measured by ELISA. WT mice challenged with Alt Ext had significantly higher levels of S100A8 in the BAL than mice mock challenged with PBS; *S100A9*$^{-/-}$ mice had no detectable S100A8, consistent with previous findings in peripheral tissues (18). S100A9 production in the lung was assessed by immunohistochemistry of lung tissue (Figures 1B and 1C). In WT mice mock challenged with PBS, S100A9 was not expressed in the respiratory epithelium, but was expressed at a low level in the alveolar epithelium and strongly expressed by type II pneumocytes. In WT mice challenged with Alt Ext, there was a marked increase in S100A9 expression in the alveolar epithelium and the airway epithelium. *S100A9*$^{-/-}$ mice did not express S100A9. Together, these results show that challenge with Alt Ext induces S1008 and S100A9 expression in the allergic lung that is not detected in *S100A9*$^{-/-}$ knockout mice.

IL-13 and Serum IgE Are Produced at Higher Levels in *S100A9*$^{-/-}$ Mice during *Alternaria*-induced Allergic Airway Inflammation

Because calprotectin production and release is induced by Alt Ext challenge, we hypothesized that calprotectin promoted allergic airway inflammation and that calprotectin-deficient *S100A9*$^{-/-}$ mice would have reduced production of type 2 cytokines. This model of allergic airway inflammation induces both innate and adaptive type 2 responses by ILC2s and Th2 cells, including producing cytokines that stimulate B cells to produce IgE (16). Surprisingly, *S100A9*$^{-/-}$ mice had similar or higher levels of type 2 cytokines in response to Alt Ext challenge. Compared with WT mice, *S100A9*$^{-/-}$ mice produced significantly higher levels of BAL IL-13 (Figure 2A), and similar levels of BAL IL-5 (Figure 2B), in response to Alt Ext challenge. *S100A9*$^{-/-}$ mice also produced significantly more serum total IgE when challenged with Alt Ext (Figure 2C). Together, these results show that *S100A9*$^{-/-}$ mice had increased IL-13 production during allergic airway inflammation, resulting in increased serum IgE.

Calprotectin-Deficient Mice Have More IL-13/IL-5–Producing $CD4^+$ T Cells during Allergic Airway Inflammation

IL-13 was detected at higher levels in Alt Ext–challenged *S100A9*$^{-/-}$ mice, suggesting that calprotectin affects ILC2 or Th2 cytokine production. To test this

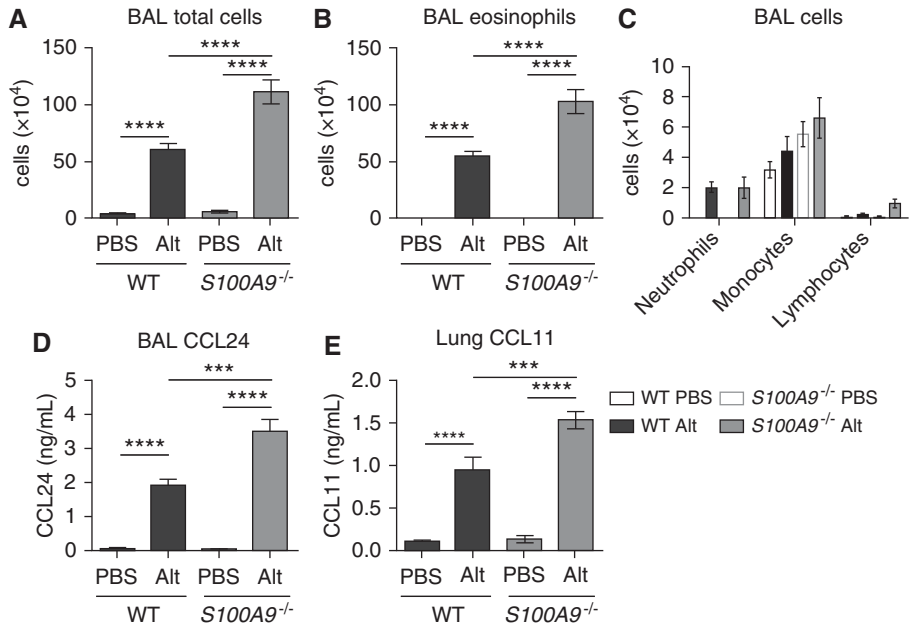

Figure 4. Mice lacking calprotectin recruit more eosinophils and produce more eotaxins when challenged with Alt. (*A*) Total BAL cells, (*B*) eosinophils, and (*C*) differential cell counts. (*D*) BAL CCL24 and (*E*) lung CCL11 were determined by ELISA. (*A–D*) Data are combined from two experiments and include 13–15 Alt-challenged and 8 or 9 mock-challenged mice per genotype. (*E*) Data are from two experiments and include 11–12 Alt-challenged and 8 or 9 mock-challenged mice per genotype. ***$P < 0.001$ and ****$P < 0.0001$. Data with error bars represent mean ± SEM.

hypothesis, the abundance of IL-13– and IL-5–producing ILC2s and Th2 cells was measured on Day 10 after Alt Ext challenge. There was no difference in IL-13– and IL-5–producing ILC2s in response to Alt Ext challenge between genotypes (Figures E3A–E3D in the data supplement). However, after gating on $CD3^+CD4^+$ T cells (Figure 3A), Alt Ext–challenged *S100A9*$^{-/-}$ mice trended toward an increase in total IL-13$^+$ Th2 cells (Figure 3B), and had significantly more total IL-5$^+$ Th2 cells (Figure 3C) and IL-13$^+$/IL-5$^+$ Th2 cells (Figure 3D). The majority of IL-5$^+$ Th2 cells were also IL-13$^+$, whereas there was a substantial population of IL-13$^+$/IL-5$^-$ Th2 cells (Figure 3A). These results are consistent with the observation of higher BAL IL-13 and serum IgE in *S100A9*$^{-/-}$ mice challenged with Alt Ext. In addition, these results reveal that calprotectin restricts the number of lung Th2 cells in response to Alt Ext challenge.

S100A9$^{-/-}$ Mice Recruit More Airway Eosinophils in Response to Alt Ext Challenge

Based on the finding that *S100A9*$^{-/-}$ mice had more IL-5–expressing Th2 cells at Day 10 of allergic airway inflammation, we hypothesized that *S100A9*$^{-/-}$ mice recruit more eosinophils to the airway in response to Alt Ext airway challenge. Therefore, we measured total cell and eosinophil numbers in the alveolar space. On Day 10 of PBS or Alt Ext challenge, BAL was harvested and total nonerythrocyte cells were counted. In addition, a portion of cells were cytocentrifuged onto glass slides for differential staining and counting of the eosinophil proportion. These experiments revealed that both WT and calprotectin-deficient *S100A9*$^{-/-}$ mice robustly recruited cells to the airway space in response to protease allergen challenge (Figure 4A), and nearly all were eosinophils (Figure 4B). As hypothesized, *S100A9*$^{-/-}$ mice challenged with Alt Ext had significantly more total cells and eosinophils harvested from their BAL. Monocytes, neutrophils, and lymphocytes in the airway space were unchanged for all four groups (Figure 4C), consistent with the conclusion that the majority of cells recruited to the airways in response to Alt Ext challenge were eosinophils.

To explain why we observed an increase in eosinophils despite equivalent IL-5 protein levels (Figure 2B), we

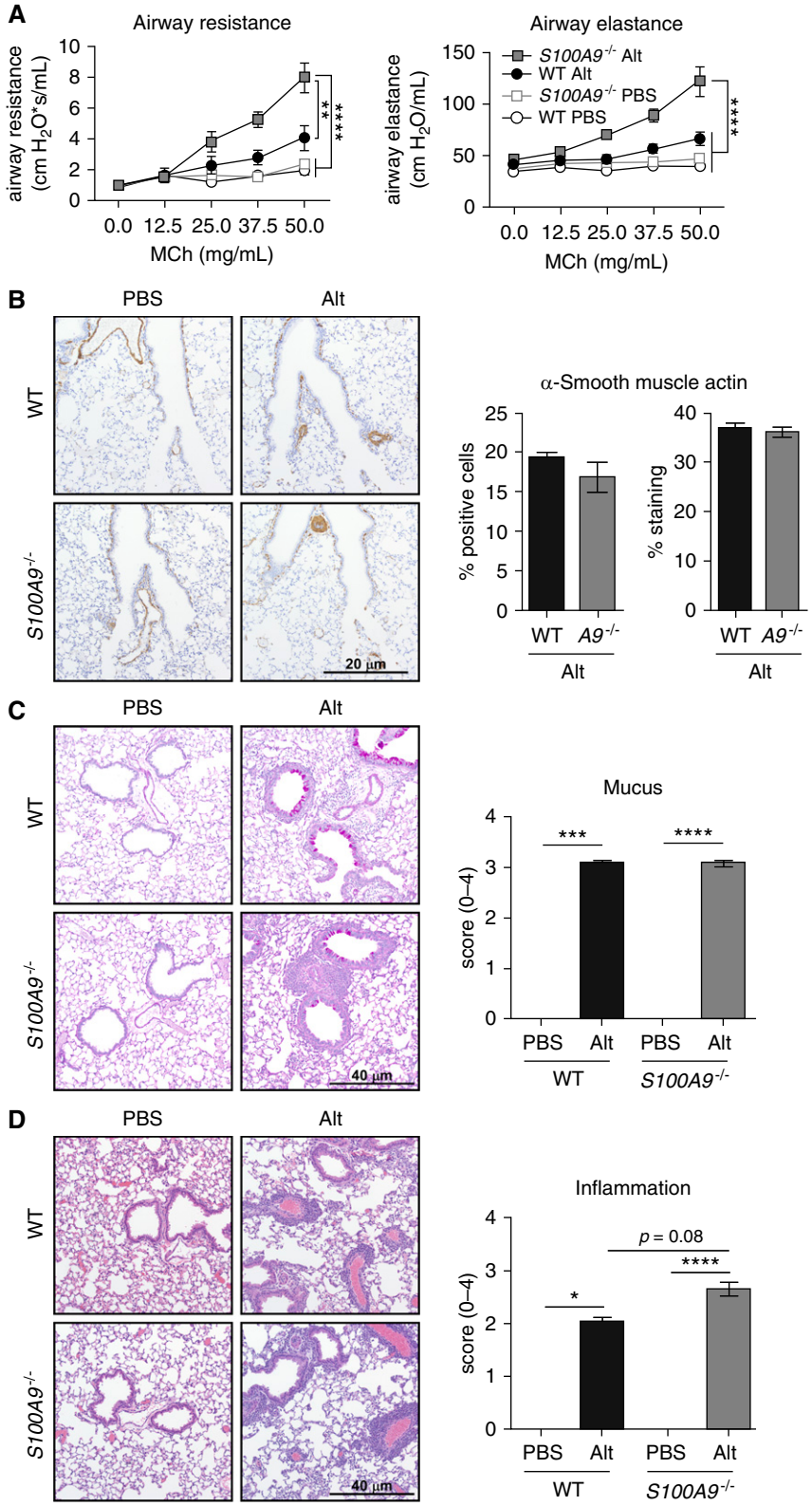

Figure 5. *S100A9*$^{-/-}$ mice have increased Alt-induced airway hyperresponsiveness, elastance, and inflammation. (*A*) Mice were challenged with increasing concentrations of methacholine (MCh) and airway resistance and elastance were measured. (*B–D*) Representative airway sections staining and quantification of α-smooth muscle actin by immunohistochemistry (*B*), mucus production by

hypothesized that eosinophil-recruiting chemokines stimulated by earlier IL-5 production may be higher in *S100A9*$^{-/-}$ mice at Day 10 of Alt Ext challenge. To test this, we measured CCL11 and CCL24 (eotaxin-1 and eotaxin-2) protein levels in the BAL and lung homogenates by ELISA. These data showed that CCL24 was significantly higher in the BAL of both WT and *S100A9*$^{-/-}$ mice challenged with Alt Ext (Figure 4D). Furthermore, among mice challenged with Alt Ext, CCL24 was significantly higher in *S100A9*$^{-/-}$ mice than in WT mice. We observed similar phenotypes of CCL11 protein levels in lung homogenates (Figure 4E). Together, these results suggest that calprotectin inhibits production of eotaxin chemokines, thereby inhibiting recruitment of eosinophils to the lung in response to airway allergen challenge.

S100A9$^{-/-}$ Mice Have Greater AHR in Response to Alt Ext Challenge

Airway remodeling and AHR are critical pathological features of asthma that lead to characteristic shortness of breath, wheezing, and chest tightness (34, 35). Due to the fact that *S100A9*$^{-/-}$ mice challenged with Alt Ext produce more IL-13 and recruit more eosinophils than WT mice, we hypothesized that *S100A9*$^{-/-}$ mice would develop greater AHR after Alt Ext challenge. On Day 10 after Alt Ext challenge, airway resistance and elastance in response to increasing methacholine concentration were measured. There was no difference in airway resistance or elastance in PBS-challenged WT or *S100A9*$^{-/-}$ mice, and there was a trend toward increased resistance and elastance in Alt Ext–challenged WT mice (Figure 5A). In contrast, there was a significant increase in airway resistance and elastance in *S100A9*$^{-/-}$ mice challenged with Alt Ext in comparison to PBS-challenged mice. Importantly, there was a significant increase in airway resistance and elastance in *S100A9*$^{-/-}$ mice compared with WT mice when both groups were challenged with Alt Ext. These data demonstrate that calprotectin protects the lung from increased airway resistance and elastance in response to allergen challenge, suggesting increased inflammation and airway remodeling in *S100A9*$^{-/-}$ mice compared with WT mice challenged with Alt Ext.

Airway remodeling includes mucus production, smooth muscle proliferation, submucosal thickening and fibrosis, and increased numbers of blood vessels (34). To identify the mechanism of increased airway resistance and elastance, serial lung sections were assessed for smooth muscle proliferation, mucus production, and inflammation. There was increased α-smooth muscle actin (SMA) staining by immunohistochemistry in response to Alt Ext in both WT and *S100A9*$^{-/-}$ mice, both qualitatively (Figure 5B) and by a semiquantitative approach (data not shown). However, among the Alt Ext–challenged mice, there was no difference in the percent SMA-positive cells or overall tissue staining based on genotype (Figure 5B). Similarly, there was significantly more mucus production by PAS staining in Alt Ext–challenged mice of both genotypes, but no difference in PAS staining between WT and *S100A9*$^{-/-}$ mice challenged with Alt Ext (Figure 5C).

Finally, airway inflammation was assessed in hematoxylin and eosin–stained tissue sections from lungs of PBS-challenged and Alt Ext–challenged WT and *S100A9*$^{-/-}$ mice. There was no inflammation in PBS-challenged WT or *S100A9*$^{-/-}$ mice, whereas there was a significant increase in inflammation in Alt Ext–challenged mice (Figure 5D). In addition, *S100A9*$^{-/-}$ mice challenged with Alt Ext had significantly increased inflammation compared with WT Alt Ext–challenged mice, including increased alveolar inflammation and eosinophilic cuffs around vessels and airways (Figure 5D). These results suggest that in calprotectin-deficient mice, increased Th2 responses stimulate airway remodeling, leading to increased airway resistance without affecting smooth muscle hyperproliferation or mucus production.

Treg Cells Comprise a Lower Proportion and Do Not Induce Expression of CD25 or FoxP3 in the Allergic Lungs of *S100A9*$^{-/-}$ Mice

Based on the finding that calprotectin-deficient *S100A9*$^{-/-}$ mice have more Th2 cells after 10 days of Alt Ext challenge, we hypothesized that calprotectin deficiency promotes Th2 responses by: *1*) enhancing release of early type 2–stimulating alarmins; *2*) serving as a DAMP or alarmin via release in the airway; or *3*) inhibiting Treg function. IL-25, TSLP, and IL-33 are epithelial-associated cytokines or alarmins that can stimulate ILC2 and Th2 cells to release type 2 cytokines, IL-4, IL-5, and IL-13 (36, 37). The model of AAI that we used is highly dependent on IL-33, whereas early production of IL-25 and TSLP is extremely low (25, 38). Consistent with previous reports, IL-25 and TSLP were below the limit of detection in the BAL at 1 hour or 6 hours after a single Alt Ext application. Similarly, TSLP in the lung homogenate at 6 hours after a single Alt Ext or PBS application was extremely low (20 pg/ml), and was only significantly induced by Alt Ext in WT mice (data not shown). To test the hypothesis that calprotectin inhibits initial IL-33 release, IL-33 was compared in BAL from WT and *S100A9*$^{-/-}$ mice 1 hour after a single Alt Ext application (Figure E3E), due to the rapid release and cleavage of IL-33 (25, 39, 40). There was no significant difference in IL-33 levels in response to Alt Ext application between WT and *S100A9*$^{-/-}$ mice, which were significantly higher than in PBS-challenged mice (Figure E3F). These data suggest that calprotectin deficiency does not affect IL-33 release in response to aeroallergen challenge.

To test the hypothesis that S100A9 deficiency abrogates Treg responses, Treg cells were quantified in WT and *S100A9*$^{-/-}$ mice. WT and calprotectin-deficient *S100A9*$^{-/-}$ mice had more CD4^{+} T cells in response Alt Ext airway challenge compared with PBS challenge, but no

Figure 5. (Continued). periodic acid–Schiff staining (*C*), and inflammation by hematoxylin and eosin staining (*D*). (*A*) Data are combined from two experiments and include 12–14 Alt-challenged and 8 mock-challenged mice per genotype. (*B*) Data represent one experiment that included eight or nine Alt-challenged and three PBS-challenged mice per genotype. (*C* and *D*) Data are combined from two experiments and include 15–17 Alt-challenged and 5 or 6 PBS-challenged mice per genotype. Significance was determined by two-way ANOVA with (*A*) Tukey's multiple comparisons and (*B*) Student's *t* test. $^{*}P < 0.05$, $^{**}P < 0.01$, $^{***}P < 0.001$, and $^{****}P < 0.0001$. Scale bars: 20 μm and 40 μm. Data with error bars represent mean ± SEM.

difference in the number or percent CD4$^+$ T cells in Alt Ext–challenged mice (Figures 6A and 6B). CD4$^+$ T cells were assessed for CD25 and FoxP3 expression to quantify the Treg cell population (Figure 6C). Among PBS-challenged mice, there was no significant difference between WT and *S100A9*$^{-/-}$ mice in total number or percent Treg cells (Figures 6D and 6E). Both WT and *S100A9*$^{-/-}$ mice recruited significantly more Treg cells when challenged with Alt Ext, and the percent Treg cells of CD4$^+$ T cells was significantly higher in Alt Ext–challenged mice (Figures 6D and 6E). These results suggest that Treg cells are recruited to control Th2 inflammation in the allergic lung. Although Alt Ext–challenged *S100A9*$^{-/-}$ and WT mice had no significant difference in total number of Treg cells, a significantly lower percentage of CD4$^+$ T cells were CD25$^+$FoxP3$^+$ in *S100A9*$^{-/-}$ mice compared with WT (Figure 6E), consistent with a greater proportion of *S100A9*$^{-/-}$ CD4$^+$ T cells being Th2 cells (Figure 3). Finally, the mean fluorescence intensity of CD25 was significantly higher in Treg cells from WT Alt Ext–challenged mice compared with mock-challenged WT or Alt Ext–challenged *S100A9*$^{-/-}$ mice (Figure 6F). Similarly, the mean fluorescence intensity of FoxP3 in Treg cells was higher in WT Alt Ext–challenged mice compared with mock-challenged mice, but was unchanged in *S100A9*$^{-/-}$ mice challenged with Alt Ext compared with mock-challenged mice (Figure 6G). Together, these data suggest that, although Treg cells in *S100A9*$^{-/-}$ animals accumulate at similar numbers, they have reduced regulatory potential and fail to control Th2-mediated inflammation.

Calprotectin Promotes WT Treg Cell Suppression of T Effector Cell Proliferation *In Vitro*

To test differences in Treg function *in vivo*, Treg cells were assessed for expression of functional markers, KLRG1, LAG3, and CTLA4, by flow cytometry. In both WT and *S100A9*$^{-/-}$ mice, expression of KLRG1, LAG3, and CTLA4 are induced in response to Alt Ext challenge, but there is no difference between the genotypes (Figures E4A–E4C). In addition, Treg function was assessed *in vivo* by measuring IL-10 in the lung homogenate. IL-10 was induced in response to Alt Ext challenge in both WT and *S100A9*$^{-/-}$ mice, but there

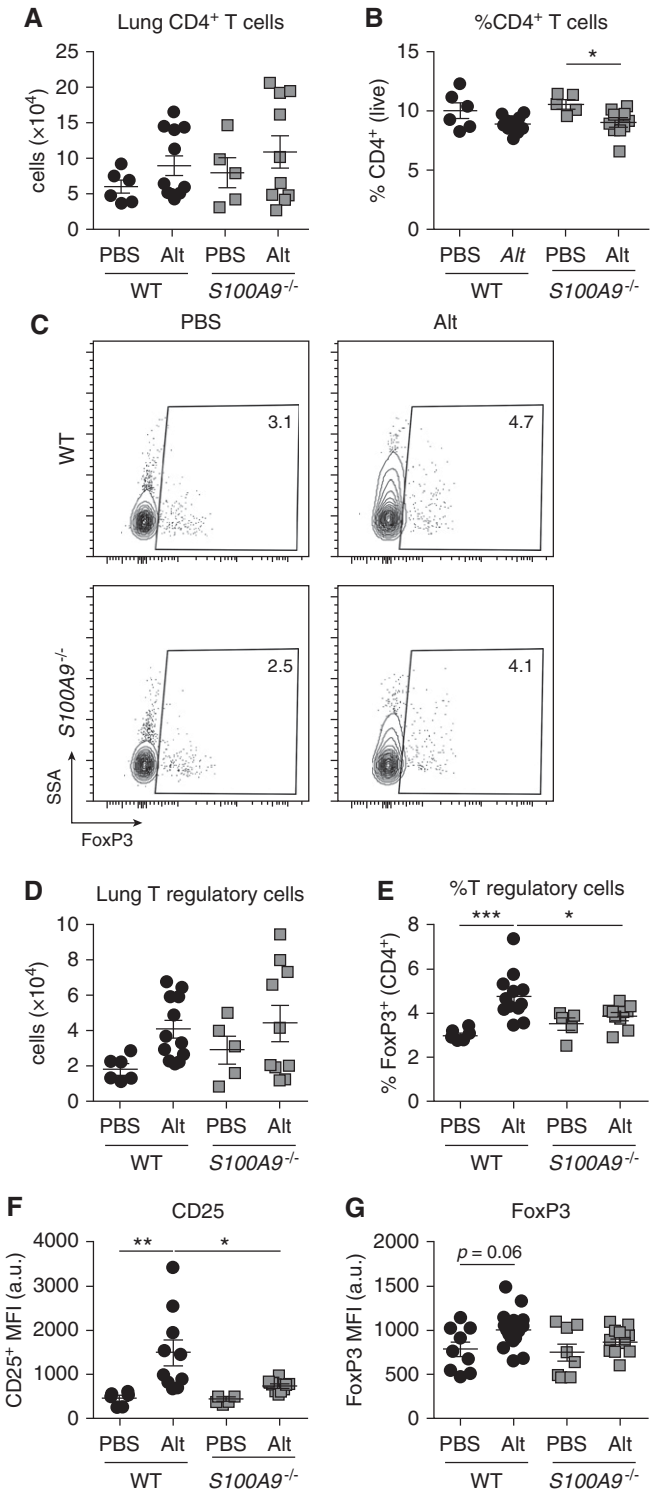

Figure 6. *S100A9*$^{-/-}$ mice have a lower proportion of T regulatory (Treg) cells and lower CD25 expression in response to Alt Ext challenge. Aggregated data for (*A*) the total number and (*B*) percent of CD4$^+$ T cells in the left lung. Representative flow plots with (*C*) percentages of the parent CD4$^+$ T cells shown, and (*D*) aggregated data for the total number and (*E*) percent of FoxP3$^+$ Treg cells. Mean fluorescence intensity (MFI) in arbitrary units (a.u.) for (*F*) CD25 and (*G*) FoxP3 of CD25$^+$FoxP3$^+$ Treg cells are reported. Data are combined from two experiments and include 10 Alt-challenged and 6 mock-challenged mice per genotype. *$P < 0.05$, **$P < 0.01$, and ***$P < 0.001$. Data with error bars represent mean ± SEM. SSA = side scatter area.

was no difference between the groups, suggesting that any differences in Treg function are IL-10 independent or rely on local differences that were not captured in whole-lung homogenates.

To test whether calprotectin directly affects Treg cell suppression, natural Treg cells were isolated from WT and *S100A9*$^{-/-}$ mice. Diluted Treg cells were incubated with purified WT CD4^{+} T effector cells labeled with CellTrace Violet and incubated for 4 days before measuring proliferation by flow cytometry. In the presence of 50 ng/ml recombinant murine calprotectin, WT Treg cells had greater suppression of CD4^{+} T effector cell proliferation than in the absence of calprotectin (Figure 7A). In contrast, *S100A9*$^{-/-}$ Treg cells displayed no difference in suppression in the presence or absence of calprotectin (Figure 7B). These results are consistent with a model where exogenous calprotectin promotes Treg suppressive activity for WT Treg cells, but not *S100A9*$^{-/-}$ Treg cells, suggesting that S100A9 and calprotectin may play multiple roles in Treg-mediated suppression of Th2 inflammation.

Discussion

Calprotectin is an important innate immune protein and comprises a major granulocyte proteome component in neutrophils and eosinophils (1, 2). Previous studies examining the role of calprotectin in allergic airway inflammation have uncovered opposing effects. To determine the overall role of calprotectin in innate and adaptive allergic airway inflammation, we challenged calprotectin-deficient mice with a clinically relevant protease allergen. *S100A9*$^{-/-}$ mice were intranasally challenged with Alt Ext in a 10-day model. These studies found that *S100A9*$^{-/-}$ mice have significantly more allergic airway inflammation, including Th2 cells and cytokine production, serum IgE production, eosinophil accumulation in the lungs, overall inflammation, and airway resistance. We further report that, although WT S100A9 protects from total airway resistance, it does not affect mucus production or airway smooth muscle hyperproliferation. The difference in total airway resistance may be due to increased eosinophilia observed in allergic *S100A9*$^{-/-}$ lungs, as eosinophils are major contributors to airway remodeling (41). Finally, calprotectin-deficient mice have similar numbers, but decreased activation state of Treg cells in the allergic lung, suggesting that Treg responses are unable to control Th2-mediated hyperinflammation in *S100A9*$^{-/-}$ mice.

Calprotectin has weak chemotactic activity, is a major component of the eosinophil proteome, and promotes neutrophil recruitment to sites of infection in a cell-intrinsic mechanism, suggesting that calprotectin-deficient mice might have lower eosinophil accumulation (2, 14, 19). However, our data demonstrate that *S100A9*$^{-/-}$ mice accumulate more eosinophils in response to aeroallergen challenge, suggesting that calprotectin-deficient eosinophils are competent at migration. Taken together, these data support a model in which *S100A9*$^{-/-}$ mice respond to Alt Ext challenge with more robust Th2 responses upstream of eosinophil chemotaxis, likely due to decreased Treg activity. These data are consistent with findings in previous models that suggest that calprotectin protects from AAI, primarily using rodent OVA models (12, 13). Interestingly, these data are in contrast to data suggesting that calprotectin promotes AAI in other studies using allergenic molds (11, 14, 15). These differences may be due to the fact that, in the present study, S100A9 protected from AAI via the adaptive immune response mediated by CD4^{+} T cells. In contrast, the studies that identified a pathogenic role for calprotectin in AAI neutralized S100A8 or S100A9 only 2 hours before a single intranasal allergen challenge in sensitized mice (14), using a neutrophilic-type asthma model (11), or in normal human bronchial epithelial cells by release of IL-25 and TSLP (15). The increased AAI in Alt Ext–challenged *S100A9*$^{-/-}$ mice reported here was mediated by CD4^{+} T cells and the adaptive immune response, which may explain the differences observed.

Importantly, these data suggest, for the first time, that there is a physiological role for calprotectin in CD4^{+} T cell responses, including Th2 and Treg cells. We did not observe differences in ILC2 number or function between WT and *S100A9*$^{-/-}$ mice at Day 10 of Alt Ext challenge, a time point at which previous studies have observed phenotypic differences based on mouse genotype (16). However, these data do not rule out a role for S100A9 in ILC2 function that affects later Th2 response by Day 10. In contrast, *S100A9*$^{-/-}$ mice had increased numbers of IL-13^{+}IL-5^{+} CD4^{+} T cells in response to Alt Ext challenge. Previous transcriptional profiling studies reported that, among CD4^{+} T cells, *S100A8* and *S100A9* are only expressed in natural Treg cells (42). Although *S100A9*$^{-/-}$ mice had similar numbers of Treg cells in the allergic lung, their activation state was abrogated. In addition, recombinant murine calprotectin promoted suppressive activity of WT Treg cells, but not *S100A9*$^{-/}$ Treg cells. Consistent with results reported here, calprotectin has been shown to promote Treg cell differentiation by signaling through CD69 and upregulation of suppressor of cytokine signaling 3 (*SOCS3*)

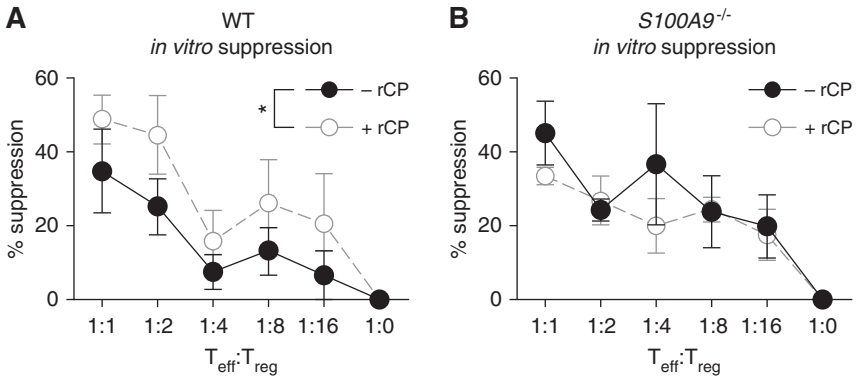

Figure 7. WT Treg cells increase suppression of T effector (T_{eff}) cell proliferation in the presence of recombinant murine calprotectin. The ability of (*A*) WT and (*B*) *S100A9*$^{-/-}$ Treg cells to suppress proliferation of WT CD4^{+} T effector cells was determined in the presence and absence of 50 ng/ml recombinant murine calprotectin (rCP). Data represent three biological replicates. $^{*}P < 0.05$. Data with error bars represent mean ± SEM.

(43). Splenic natural Treg cells from C57BL/6 mice express calprotectin receptors, RAGE and CD69 (42, 44), suggesting that calprotectin released during AAI may signal directly on Treg cells in the allergic lung. Together, these findings suggest that S100A9 and/or calprotectin play a role in Treg cell activation, perhaps both extrinsically and intrinsically.

Together, these studies identify S100A9 as protective from type 2 inflammation in response to challenge from Alt Ext. Specifically, these studies uncover a role for S100A9 and/or calprotectin in adaptive immune inflammation, because *S100A9*$^{-/-}$ mice challenged with Alt Ext produce more serum IgE, accumulate more Th2 cells in the lung, and have reduced Treg activation. Future studies defining the role of calprotectin in Treg function and release in response to protease aeroallergens will clarify its role in CD4^{+} T cell function during allergic airway inflammation. Calprotectin has been previously described as a proinflammatory DAMP that amplifies the innate immune response (5, 6). In contrast, the finding that calprotectin protects from allergic airway inflammation via modulating the adaptive immune response suggest that calprotectin is also antiinflammatory. Consistent with an antiinflammatory role for calprotectin, a recent study found that calprotectin programs neonatal innate immunity to prevent hyperinflammation and protect from sepsis (45). In addition, S100A9 stimulates myeloid-derived suppressor cell production associated with cancer and suppression of antitumor immune responses (46). Together with the results reported in this work, these findings suggest that calprotectin promotes immunoregulatory function to prevent hyperinflammation. ■

Author disclosures are available with the text of this article at www.atsjournals.org.

Acknowledgment: The authors thank members of the Skaar laboratory for critical reading of the manuscript, Allison Norlander for helpful discussion, Sergey Novitskiy for α-FoxP3 antibody, Ly Pham and Michael Noto for assistance with the IL-10 ELISA, and David Flaherty, Christian Warren, and Brittany Matlock of the Vanderbilt Flow Cytometry Shared Resource for assistance.

References

1. Stríz I, Trebichavský I. Calprotectin: a pleiotropic molecule in acute and chronic inflammation. *Physiol Res* 2004;53:245–253.
2. Wilkerson EM, Johansson MW, Hebert AS, Westphall MS, Mathur SK, Jarjour NN, *et al*. The peripheral blood eosinophil proteome. *J Proteome Res* 2016;15:1524–1533.
3. Zackular JP, Chazin WJ, Skaar EP. Nutritional immunity: S100 proteins at the host-pathogen interface. *J Biol Chem* 2015;290:18991–18998.
4. Palmer LD, Skaar EP. Transition metals and virulence in bacteria. *Annu Rev Genet* 2016;50:67–91.
5. Ehrchen JM, Sunderkötter C, Foell D, Vogl T, Roth J. The endogenous Toll-like receptor 4 agonist S100A8/S100A9 (calprotectin) as innate amplifier of infection, autoimmunity, and cancer. *J Leukoc Biol* 2009;86:557–566.
6. Chan JK, Roth J, Oppenheim JJ, Tracey KJ, Vogl T, Feldmann M, *et al*. Alarmins: awaiting a clinical response. *J Clin Invest* 2012;122:2711–2719.
7. Vogl T, Tenbrock K, Ludwig S, Leukert N, Ehrhardt C, van Zoelen MA, *et al*. Mrp8 and Mrp14 are endogenous activators of Toll-like receptor 4, promoting lethal, endotoxin-induced shock. *Nat Med* 2007;13:1042–1049.
8. Aoki T, Matsumoto Y, Hirata K, Ochiai K, Okada M, Ichikawa K, *et al*. Expression profiling of genes related to asthma exacerbations. *Clin Exp Allergy* 2009;39:213–221.
9. Gray RD, MacGregor G, Noble D, Imrie M, Dewar M, Boyd AC, *et al*. Sputum proteomics in inflammatory and suppurative respiratory diseases. *Am J Respir Crit Care Med* 2008;178:444–452.
10. Lee TH, Jang AS, Park JS, Kim TH, Choi YS, Shin HR, *et al*. Elevation of S100 calcium binding protein A9 in sputum of neutrophilic inflammation in severe uncontrolled asthma. *Ann Allergy Asthma Immunol* 2013;111:268–275.e1.
11. Lee TH, Chang HS, Bae DJ, Song HJ, Kim MS, Park JS, *et al*. Role of S100A9 in the development of neutrophilic inflammation in asthmatics and in a murine model. *Clin Immunol* 2017;183:158–166.
12. Zhao J, Endoh I, Hsu K, Tedla N, Endoh Y, Geczy CL. S100A8 modulates mast cell function and suppresses eosinophil migration in acute asthma. *Antioxid Redox Signal* 2011;14:1589–1600.
13. Yin LM, Li HY, Zhang QH, Xu YD, Wang Y, Jiang YL, *et al*. Effects of S100A9 in a rat model of asthma and in isolated tracheal spirals. *Biochem Biophys Res Commun* 2010;398:547–552.
14. Greenlee KJ, Corry DB, Engler DA, Matsunami RK, Tessier P, Cook RG, *et al*. Proteomic identification of *in vivo* substrates for matrix metalloproteinases 2 and 9 reveals a mechanism for resolution of inflammation. *J Immunol* 2006;177:7312–7321.
15. Kato T, Kouzaki H, Matsumoto K, Hosoi J, Shimizu T. The effect of calprotectin on TSLP and IL-25 production from airway epithelial cells. *Allergol Int* 2017;66:281–289.
16. Oczypok EA, Milutinovic PS, Alcorn JF, Khare A, Crum LT, Manni ML, *et al*. Pulmonary receptor for advanced glycation end-products promotes asthma pathogenesis through IL-33 and accumulation of group 2 innate lymphoid cells. *J Allergy Clin Immunol* 2015;136:747–756, e4.
17. Hammad H, Chieppa M, Perros F, Willart MA, Germain RN, Lambrecht BN. House dust mite allergen induces asthma via Toll-like receptor 4 triggering of airway structural cells. *Nat Med* 2009;15:410–416.
18. Manitz MP, Horst B, Seeliger S, Strey A, Skryabin BV, Gunzer M, *et al*. Loss of S100A9 (MRP14) results in reduced interleukin-8-induced CD11b surface expression, a polarized microfilament system, and diminished responsiveness to chemoattractants *in vitro*. *Mol Cell Biol* 2003;23:1034–1043.
19. Juttukonda LJ, Berends ETM, Zackular JP, Moore JL, Stier MT, Zhang Y, *et al*. Dietary manganese promotes staphylococcal infection of the heart. *Cell Host Microbe* 2017;22:531–542, e8.
20. Hood MI, Mortensen BL, Moore JL, Zhang Y, Kehl-Fie TE, Sugitani N, *et al*. Identification of an *Acinetobacter baumannii* zinc acquisition system that facilitates resistance to calprotectin-mediated zinc sequestration. *PLoS Pathog* 2012;8:e1003068. [Published erratum appears in *PLoS Pathog* 9.]
21. Corbin BD, Seeley EH, Raab A, Feldmann J, Miller MR, Torres VJ, *et al*. Metal chelation and inhibition of bacterial growth in tissue abscesses. *Science* 2008;319:962–965.
22. Zaia AA, Sappington KJ, Nisapakultorn K, Chazin WJ, Dietrich EA, Ross KF, *et al*. Subversion of antimicrobial calprotectin (S100A8/S100A9 complex) in the cytoplasm of TR146 epithelial cells after invasion by *Listeria monocytogenes*. *Mucosal Immunol* 2009;2:43–53.
23. Achouiti A, Vogl T, Urban CF, Röhm M, Hommes TJ, van Zoelen MA, *et al*. Myeloid-related protein-14 contributes to protective immunity in gram-negative pneumonia derived sepsis. *PLoS Pathog* 2012;8:e1002987.
24. Agarwal R. Severe asthma with fungal sensitization. *Curr Allergy Asthma Rep* 2011;11:403–413.
25. Doherty TA, Khorram N, Chang JE, Kim HK, Rosenthal P, Croft M, *et al*. STAT6 regulates natural helper cell proliferation during lung inflammation initiated by *Alternaria*. *Am J Physiol Lung Cell Mol Physiol* 2012;303:L577–L588.
26. Zhou W, Toki S, Zhang J, Goleniewksa K, Newcomb DC, Cephus JY, *et al*. Prostaglandin I_2 signaling and inhibition of group 2 innate lymphoid cell responses. *Am J Respir Crit Care Med* 2016;193:31–42.

27. Toki S, Goleniewska K, Reiss S, Zhou W, Newcomb DC, Bloodworth MH, *et al*. The histone deacetylase inhibitor trichostatin A suppresses murine innate allergic inflammation by blocking group 2 innate lymphoid cell (ILC2) activation. *Thorax* 2016;71:633–645.
28. Valladao AC, Frevert CW, Koch LK, Campbell DJ, Ziegler SF. STAT6 regulates the development of eosinophilic versus neutrophilic asthma in response to *Alternaria alternata*. *J Immunol* 2016;197:4541–4551.
29. Cephus JY, Stier MT, Fuseini H, Yung JA, Toki S, Bloodworth MH, *et al*. Testosterone attenuates group 2 innate lymphoid cell–mediated airway inflammation. *Cell Reports* 2017;21:2487–2499.
30. van den Brûle S, Heymans J, Havaux X, Renauld JC, Lison D, Huaux F, *et al*. Profibrotic effect of IL-9 overexpression in a model of airway remodeling. *Am J Respir Cell Mol Biol* 2007;37:202–209.
31. Causton B, Pardo-Saganta A, Gillis J, Discipio K, Kooistra T, Rajagopal J, *et al*. CARMA3 mediates allergic lung inflammation in response to *Alternaria alternata*. *Am J Respir Cell Mol Biol* 2018;59:684–694.
32. Passey RJ, Williams E, Lichanska AM, Wells C, Hu S, Geczy CL, *et al*. A null mutation in the inflammation-associated S100 protein S100A8 causes early resorption of the mouse embryo. *J Immunol* 1999;163: 2209–2216.
33. Newcomb DC, Boswell MG, Huckabee MM, Goleniewska K, Dulek DE, Reiss S, *et al*. IL-13 regulates Th17 secretion of IL-17A in an IL-10 dependent manner. *J Immunol* 2012;188:1027–1035.
34. Fahy JV. Type 2 inflammation in asthma: present in most, absent in many. *Nat Rev Immunol* 2015;15:57–65.
35. Lambrecht BN, Hammad H. The immunology of asthma. *Nat Immunol* 2015;16:45–56.
36. Divekar R, Kita H. Recent advances in epithelium-derived cytokines (IL-33, IL-25, and thymic stromal lymphopoietin) and allergic inflammation. *Curr Opin Allergy Clin Immunol* 2015;15:98–103.
37. Martin NT, Martin MU. Interleukin 33 is a guardian of barriers and a local alarmin. *Nat Immunol* 2016;17:122–131.
38. Bartemes KR, Iijima K, Kobayashi T, Kephart GM, McKenzie AN, Kita H. IL-33–responsive lineage^{-}CD25^{+} CD44^{hi} lymphoid cells mediate innate type 2 immunity and allergic inflammation in the lungs. *J Immunol* 2012;188:1503–1513.
39. Kouzaki H, Iijima K, Kobayashi T, O'Grady SM, Kita H. The danger signal, extracellular ATP, is a sensor for an airborne allergen and triggers IL-33 release and innate Th2-type responses. *J Immunol* 2011;186:4375–4387.
40. Snelgrove RJ, Gregory LG, Peiro T, Akthar S, Campbell GA, Walker SA, *et al*. *Alternaria*-derived serine protease activity drives IL-33-mediated asthma exacerbations. *J Allergy Clin Immunol* 2014;134: 583–592.e6.
41. Humbles AA, Lloyd CM, McMillan SJ, Friend DS, Xanthou G, McKenna EE, *et al*. A critical role for eosinophils in allergic airways remodeling. *Science* 2004;305:1776–1779.
42. Stubbington MJ, Mahata B, Svensson V, Deonarine A, Nissen JK, Betz AG, *et al*. An atlas of mouse CD4^{+} T cell transcriptomes. *Biol Direct* 2015;10:14.
43. Lin CR, Wei TY, Tsai HY, Wu YT, Wu PY, Chen ST. Glycosylation-dependent interaction between CD69 and S100A8/S100A9 complex is required for regulatory T-cell differentiation. *FASEB J* 2015;29: 5006–5017.
44. Heng TS, Painter MW; Immunological Genome Project Consortium. The Immunological Genome Project: networks of gene expression in immune cells. *Nat Immunol* 2008;9:1091–1094.
45. Ulas T, Pirr S, Fehlhaber B, Bickes MS, Loof TG, Vogl T, *et al*. S100-alarmin–induced innate immune programming protects newborn infants from sepsis. *Nat Immunol* 2017;18:622–632.
46. Cheng P, Corzo CA, Luetteke N, Yu B, Nagaraj S, Bui MM, *et al*. Inhibition of dendritic cell differentiation and accumulation of myeloid-derived suppressor cells in cancer is regulated by S100A9 protein. *J Exp Med* 2008;205:2235–2249.

The innate immune protein S100A9 protects from Th2-mediated allergic airway inflammation

Lauren D. Palmer Ph.D., K. Nichole Maloney M.S., Kelli L. Boyd D.V.M., Ph.D. ,

A. Kasia Goleniewska M.S., Shinji Toki Ph.D., Christina N. Maxwell, Walter J. Chazin,

R. Stokes Peebles Jr., Dawn C. Newcomb Ph.D., and Eric P. Skaar Ph.D., M.P.H.

ONLINE DATA SUPPLEMENT

Supplementary Information

METHODS

Histopathology of lungs

Tissue sections (5 µm) were stained with hematoxylin and eosin stain to assess inflammation, or periodic acid-Schiff (PAS) to assess mucus cell metaplasia as a measure of mucin expression. Immunohistochemistry staining was performed using the Leica BOND-MAX autostainer (Wetzlar, Germany). Lung S100A9 production was assessed by immunohistochemistry staining with Cell Signaling Technologies clone D3U8M (Danvers, MA). To assess smooth muscle hypertrophy and hyperplasia, immunohistochemistry staining for □-smooth muscle actin (SMA) with Abcam ab7817 (Cambridge, United Kingdom) was performed. Slides were examined and scored by a pathologist who was blinded to the experimental groups. S100A9 was scored according to the following scale: 0, no staining; 1, normal staining of type II pneumocytes only; 2, staining of type II pneumocytes and all alveolar epithelium with mild intensity; 3, staining of type II pneumocytes and all alveolar epithelium with moderate intensity; 4, staining of type II pneumocytes and all alveolar epithelium with marked intensity.

Inflammation was scored according to the following scale: 0, no inflammatory infiltrates observed in the examined sections; 1, rare perivascular inflammatory infiltration; 2, few perivascular inflammatory infiltrates with rare extenstion into the interstitium; 3, moderate perivascular inflammatory infiltration and with multifocal interstitial infiltration; 4, marked perivascular inflammatory infiltrates with extensive involvement of the interstitium and alveolar spaces. Mucus production was scored according to the following scale: 0, PAS positive cell are not observed in the examined sections; 1, less than 10% of cells in medium and small airways are PAS positive; 2, 10-20% PAS positive cells in medium and small airways; 3, greater than 20%

cells in medium and small airways are PAS positive and hyperplasia of PAS positive cells is observed; 4, greater than 20% PAS positive cells in medium and small airways, hyperplasia of PAS positive cells and mucous plugging of airways. Immunohistochemistry (IHC) anti-SMA slides were digitally scanned on a Leica SCN400 Slide Scanner and quantified for % positive cells and % positive total tissue area using Ariol analysis scripts (Leica).

Flow cytometry staining

Right lungs were digested to single cell suspensions with 1 mg/mL collagenase type I and 0.1 mg/mL DNase. Digestion was stopped by the addition of EDTA to 1 mM. Digested lungs were passed through a 70-μm filter and treated with red blood cell lysis buffer (BioLegend, San Diego, CA). Cells were restimulated with 50 ng/mL PMA, 1 μg/mL ionomycin, and 0.07% golgi stop for 6 hours at 37°C in RPMI + 10% FBS. Meanwhile, live cells were counted by trypan blue exclusion on a hemocytometer. Following restimulation, 2 million lung cells were stained with viability dye from Tonbo (San Diego, CA), blocked with an anti-FcR antibody (clone 2.4G2), and stained with antibodies listed in Table E1. Th2 cells were surface stained with anti-CD90, anti-CD45, anti-CD4, anti-CD3, and anti-FCεR1. ILC2 cells were surface stained with anti-Lineage cocktail, anti-CD3, anti-CD25, anti-CD127, anti-CD45, and anti-ST2. After washing, ILC2 cells were stained with fluorochrome-labeled streptavidin. Cells were then fixed and permeabilized using FoxP3 Fix/Perm Buffer Set by BioLegend and intracellularly stained with anti-IL-5 and anti-IL-13. Th2 cells were pre-gated as $CD90^{+}CD45^{+}CD3^{+}CD4^{+}$ and assessed for IL-5 and IL-13 staining (Fig. S1A). ILC2s were pre-gated as $lineage^{-}CD3^{-}CD45^{+}$ $ST2^{+}CD127^{+}$ and assessed for IL-5 and IL-13 staining (Fig. S1B). T regulatory (Treg) cells were quantified from left lungs on day 10 following BAL. Left lungs were digested to single cell suspensions, and 2 million cells were stained for viability (Tonbo, San Diego, CA), surface stained for CD4 and CD25, fixed and permeabilized as

above, and intracellularly stained with anti-FoxP3. T regulatory cells were pre-gated as $CD4^+FoxP3^+$ and assessed for CD25 and FoxP3 (Fig. S2A). Differences in Treg proportion and CD25 expression were confirmed in littermate controls (one experiment shown in Fig. 6). Flow analysis was conducted on LSRII or Fortessa flow cytometers by BD Biosciences (San Jose, CA), and all data was processed using FlowJo software by FlowJo LLC (Ashland, OR).

Methacholine challenge

Airway hyperresponsiveness (AHR) and airway elastance (AE) was measured on day 10 after Alt Ext challenge. Each mouse was anesthetized by pentobarbital and the trachea was cannulated with a 20-gauge metal stub adapter. The animal was placed on a FlexiVent small-animal ventilator (SCIREQ, Montreal, Canada), with 150 breaths/min and a tidal volume of 10 mL/kg of body weight. Airway responsiveness was assessed by administering incremental concentrations of aerosolized methacholine (0, 12.5, 25, 37.5, and 50 mg/mL in saline) via an Aeroneb in-line ultra-nebulizer (SCIREQ, Montreal, Canada). The SCIREQ software calculates the respiratory system resistance (Rrs in cm H_2O*s/mL) by dividing the change in pressure by the change in flow from single frequency forced oscillation technique; elastance (Ers in cm H_2O/mL) captures the elastic stiffness and is reciprocal of compliance.

In vitro T regulatory cell suppression assay

Wild-type $CD4^+CD25^-$ T effector (Teff) cells and $CD4^+CD25^-$ Treg cells were isolated using the $CD4^+CD25^+$ Regulatory T Cell Isolation Kit for mouse from Miltenyi Biotec Inc. (Auburn, CA). Sorting buffer was RPMI + 1% FBS, and complete medium was RPMI + 10% FBS + 1% penicillin/streptomycin + 1% sodium pyruvate + 1% non-essential amino acids. Wild-type Teff cells were labeled with CellTrace Violet from Invitrogen (Carlsbad, CA) in PBS for 20 min at 37°C and the dye reaction was quenched with complete medium. Wild-type Teff cells were

incubated with either wild-type or *S100A9*$^{-/-}$ Treg cells at the indicated ratios for 4 days prior to staining with anti-CD4 PE-Cy7 as for Treg cells above, with and without endotoxin-free recombinant murine calprotectin. Anti-CD3 (1 μg/mL) and anti-CD28 (4 μg/mL) included to stimulate Teff proliferation were Ultra-LEAF purified from Biolegend (San Diego, CA). Teff proliferation was assessed on single cells following the gating scheme outlined in Fig. S2B. Percent suppression was calculated as 100 X ((%divided Teff no Treg)-(%divided Teff with Treg))/(%divided Teff no Treg).

Table E1. Flow cytometry antibodies.

Epitope	Clone	Manufacturer	Fluorophore	Dilution
CD90	353-2.1	BD Horizon	BV786	1:1250
CD45	30-F11	eBioscience	AF700	1:1250
CD4	H129.19	BD Pharmingen	FITC	1:500
CD3	145-2C11		Pacific Blue	1:500
FcεR1	MAR-1	eBioscience	PE-Cy7	1:500
Lineage cocktail	130-092-613	Miltenyi Biotec	biotin	1:100
CD3	17A2	eBioscience	biotin	1:500
	Streptavidin	BD Pharmingen	APC-Cy7	1:1000
CD25	PC61.5	eBioscience	AF488	1:125 (ILC2); 1:1667 (Treg)
CD127	A7R34	eBioscience	PE-Cy7	1:250
CD45	30-F11	eBioscience	AF700	1:250
ST2	eBio927	eBioscience	PerCP-eFluor 710	1:357
IL-5	TRFK5	BD Biosciences	APC	1:67
IL-13	eBio13A	eBioscience	PE	1:67
CD4	RM4-5	BD Biosciences	PE-Cy7	1:1667
FoxP3	FJK-16S	eBioscience	APC	1:100
KLRG1	2F1/KLRG1	Biolegend	PE/Dazzle™ 594	1:200
LAG3	C9B7W	BD Biosciences	BV786	1:100
CTLA4	UC10-4B9	Biolegend	APC	1:50

SUPPLEMENTARY FIGURES AND LEGENDS

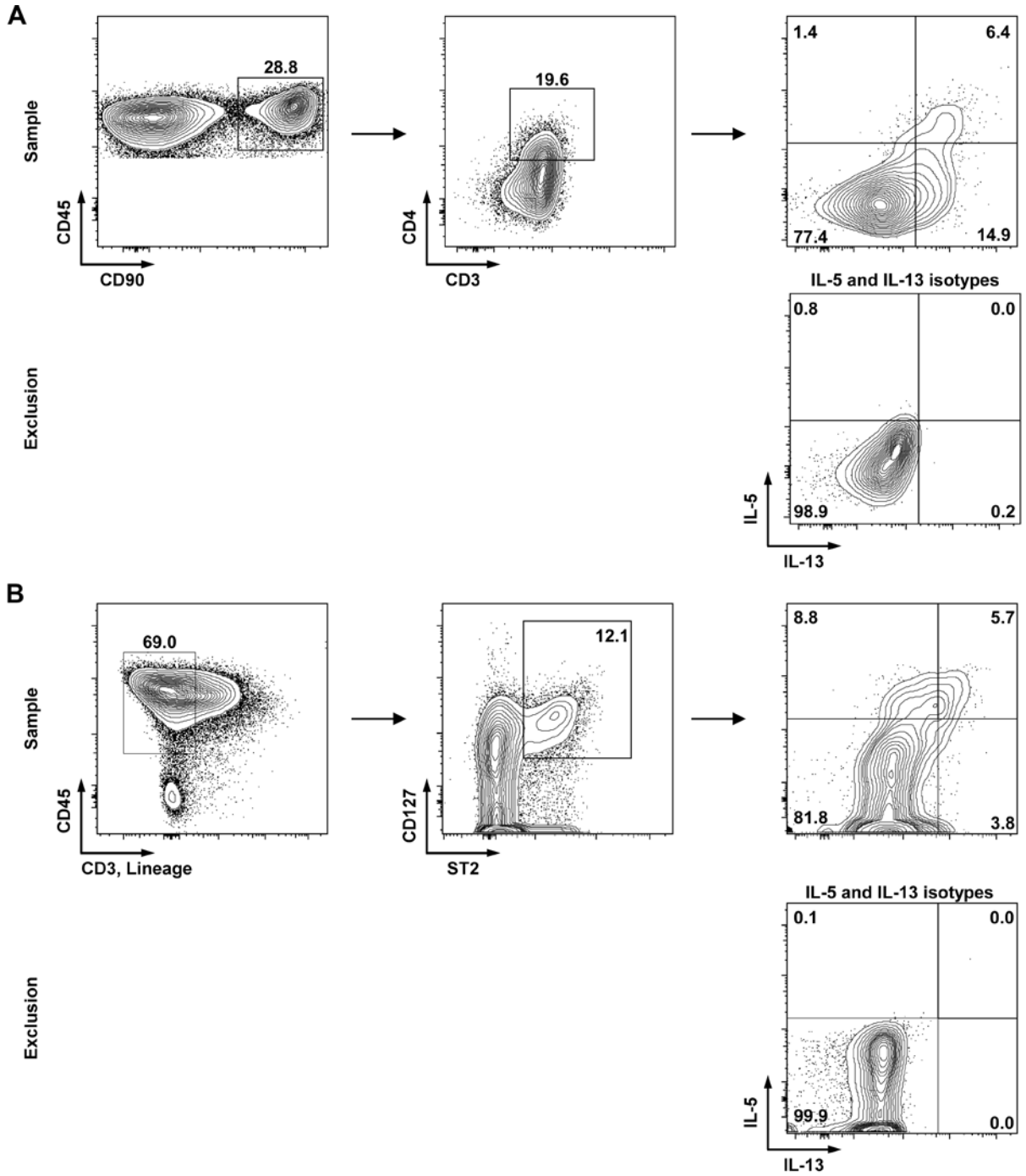

Figure E1: Gating strategies for Th2 cells and ILC2. Data are representative of the gating strategy used to quantify Th2 cells (**A**) and group 2 innate lymphoid cells (**B**).

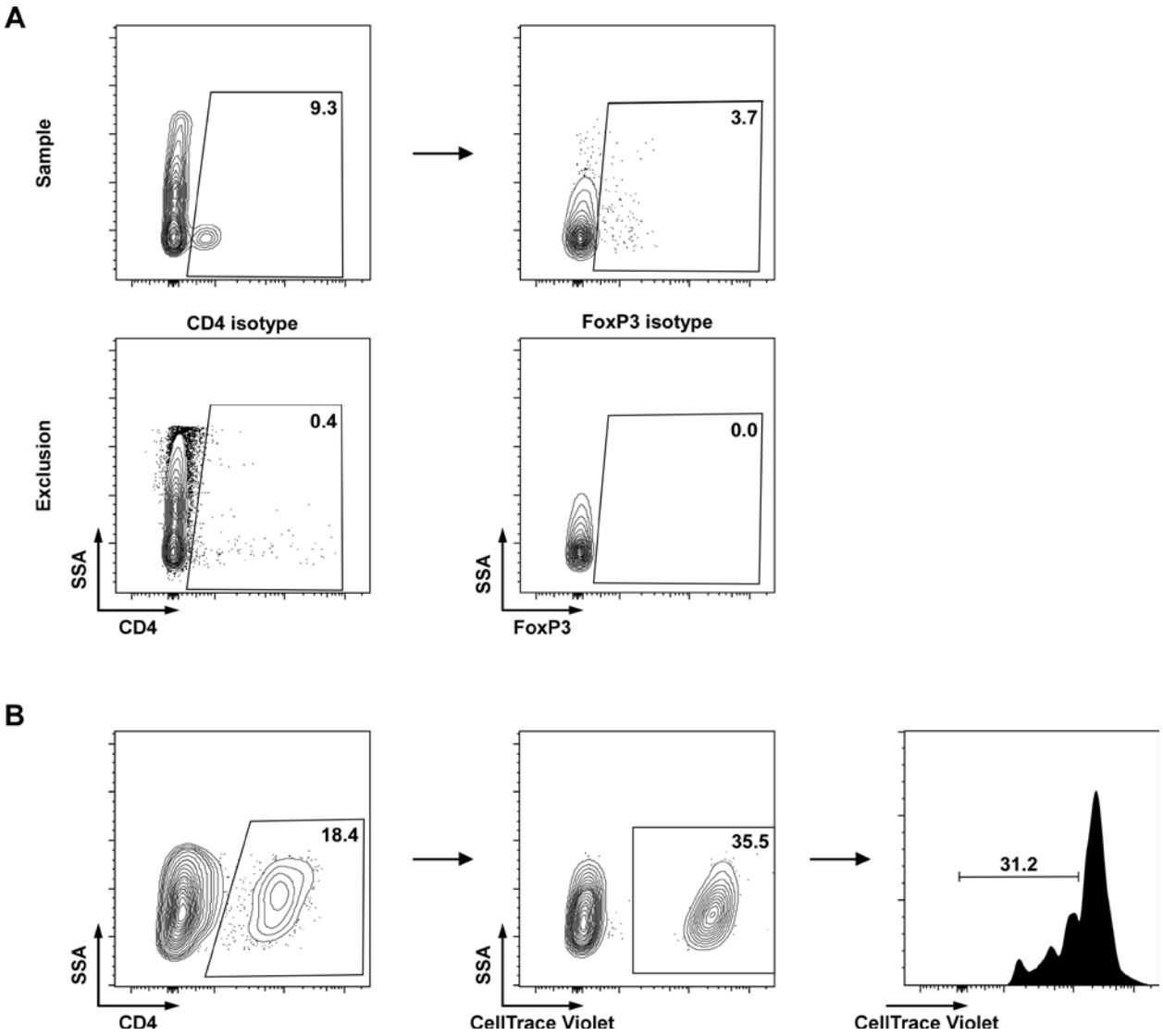

Figure E2: Gating strategies for T regulatory cells. (**A**) Data are representative of the gating strategy used to quantify T regulatory cells in the lungs. (**B**) Data are representative of the gating strategy used to quantify T regulatory cell suppression of T effector cell proliferation in vitro.

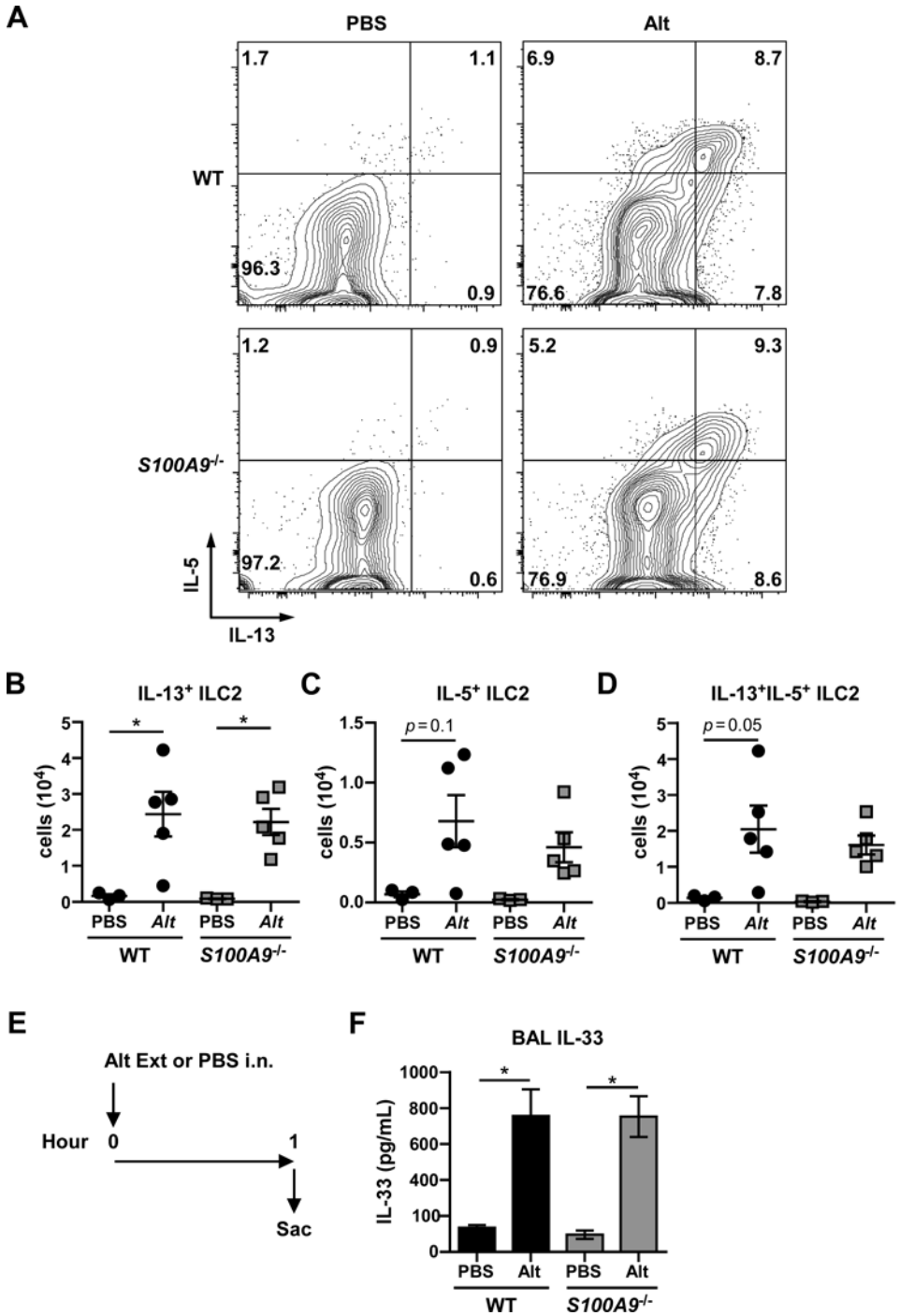

Figure E3: Wild-type and *S100A9*$^{-/-}$ mice have no difference in group 2 innate lymphoid cell (ILC2) numbers or IL-33 release in response to Alt Ext. Representative flow plots with percentages of the parent ST2^{+}CD127^{+} ILC2s shown (**A**), and aggregated data for the total number of (**B**) IL-13^{+}, (**C**) IL-5^{+}, and (**D**) IL-13^{+}IL-5^{+} double positive ILC2s. (**B-D**) Data are representative of three experiments and include 5 Alt Ext challenged and 3 mock challenged mice per genotype. (**E**) Mice were challenged with Alt Ext or mock challenged with PBS at hour 0 and humanely euthanized 1 h later. (**F**) IL-33 was measured in BAL. Data are from one experiment with 9-10 Alt Ext challenged and 4-5 mock challenged mice per genotype.

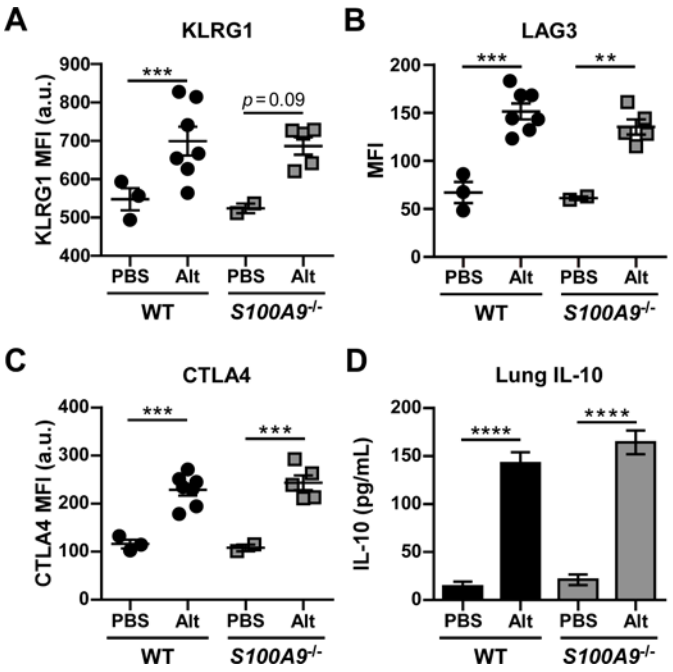

Figure E4: Wild-type and *S100A9*$^{-/-}$ mice have no difference in Treg functional markers or IL-10 production in response to Alt Ext. Wild-type and *S100A9*$^{-/-}$ were challenged with Alt Ext or mock challenged with PBS and humanely euthanized on day 10. Expression of lung Treg functional markers on CD4+Foxp3+ Treg cells were assessed by flow cytometry, including KLRG1 (**A**), LAG3 (**B**), and CTLA4 (**C**) IL-5^{+}. (**D**) IL-10 was measured in lung tissue homogenate by ELISA; data represent 3 mock-challenged mice and 5 Alt Ext challenged mice.